

and $u_F = k_F/m$, we have:

$$\sigma = (n_e e^2 / m) \tau \quad (8-16)$$

where,

$$\frac{1}{\tau} = 2[\Gamma(k_F) - \Gamma'(k_F)] = 2\pi n_e \frac{k_F}{m} \int_0^\pi \sigma(\theta) \times (1 - \cos\theta) \sin\theta d\theta, \quad (8-17)$$

and $\sigma(\theta)$ is the differential scattering cross section for an electron of momentum k_F .

Equation (8-16) is the standard classical expression for the conductivity. Γ , the decay rate for the single-particle state, is the usual "scattering-out" probability; and Γ' turns out to be the "scattering-in" term. Note that there is no effect of the exclusion principle remaining even in the calculation of $\sigma(\theta)$ in (8-17). $\sigma(\theta)$

is the exact cross section for a free electron scattered by an isolated impurity center. This happened mathematically because we defined the poles in t^+ by keeping ω always just above the real axis.

In similar fashion, it should be possible to rewrite (8-15) in terms of a scattering cross section for effective electrons scattered by shielded impurities. This would involve finding the correct normalization for these scattering states (see Van Hove¹⁴), and it seems simplest, even if a bit less physical, to keep (8-15) in its present form.

ACKNOWLEDGMENT

The author wishes to thank Professor Walter Kohn for suggesting this investigation and for several helpful discussions.

Electro-Optic Kerr Effect and Polarization Reversal in Deuterium-Doped Rochelle Salt

H. H. WIEDER AND D. A. COLLINS
U. S. Naval Ordnance Laboratory, Corona, California
(Received June 30, 1960)

Polarization reversal as a function of nucleation and growth of domains in ferroelectric deuterium-doped Rochelle salt was investigated by means of the electro-optic Kerr effect. The results indicate that a phenomenological model based on statistical nucleation of domains in a plane including the ferroelectric axis followed by a two-dimensional sidewise expansion of the domains, will adequately account for the experimental observations for fields larger than 50 volts/cm. For lower fields, the process is controlled primarily by the nucleation of new domains due to localized stresses which hinder the displacement of domain walls.

1. INTRODUCTION

A STUDY of the polarization process in Rochelle salt (RS) was undertaken for a dual purpose. First, some features of polarization reversal interpreted as the nucleation and motion of antiparallel domains have only been partially investigated. Second, the validity of a phenomenological model for the reversal mechanism was to be tested on a ferroelectric crystal in which domain dynamics could be discerned optically, under polarized light, as well as electrically, from a study of the displacement current transients.

The displacement current parameters predicted from this model were shown to be in excellent agreement with experiment in the case of colemanite.¹ No direct visual observations could be made however, which might provide additional justification for the choice of a reversal mechanism based only on nucleation and subsequent sidewise expansion of domains. Two-dimensional wall displacement was observed in barium

titanate²⁻⁴ under restricted experimental conditions and some features of the above model were confirmed. Rochelle salt, however, offers because of its large electro-optic effects, the advantage of unrestricted observations of electrical and optical features of the polarization reversal process.

Mitsui and Furuichi⁵ studied the domain structure and domain dynamics of Rochelle salt showing that the spontaneous shear deformation between neighboring domains causes the optical indicatrix to turn in opposite directions about the a axis leading to a difference in extinction positions between adjacent domains. Indenbom and Chernysheva⁶ discussed the monoclinicity of Rochelle salt using quantitative measurements of the turning angle of the optical indicatrix to define a thermodynamic potential theory analogous

² R. C. Miller, Phys. Rev. **111**, 736 (1958).

³ R. C. Miller and A. Savage, Phys. Rev. **112**, 755 (1958).

⁴ R. C. Miller and A. Savage, Phys. Rev. **115**, 1176 (1959).

⁵ T. Mitsui and J. Furuichi, Phys. Rev. **90**, 193 (1953).

⁶ V. L. Indenbom and M. A. Chernysheva, Kristallografiya **2** (1957) [translation: Soviet Phys.-Cryst. **2**, 522 (1957)].

¹ H. H. Wieder, J. Appl. Phys. **31**, 180 (1960).

to constructions based on the polarization as the temperature variable parameter. They established the direct proportionality between the spontaneous polarization and the angle of rotation. Similar results were obtained by Abe⁷ whose investigations indicate that not only the spontaneous polarization, but also the change in polarization, during reversal of the remanent polarization might be proportional to its electro-optic analog effect. Wieder⁸ investigated the displacement current transients obtained during switching and described the dependence of the significant parameters of these transients upon applied field and temperature in the ferroelectric range. The fast reversal time was proposed to be due to nucleation and domain wall displacement in the direction of the ferroelectric a axis.

The experimental investigations to be described subsequently were undertaken to test, by means of the Kerr electro-optic effect, the relevance of phenomenological theories of polarization reversal such as proposed for BaTiO₃⁹ and in modified form shown to apply to ferroelectric colemanite,¹ to the nucleation and domain dynamics present in Rochelle salt.

2. EXPERIMENTAL

Experimental investigations on RS in the ferroelectric phase are difficult because close control of ambient temperature and humidity are required and the low Curie temperature generally necessitates some refrigeration.

It was decided, therefore, to take advantage of the isotope effect in RS by partial replacement of hydrogen with deuterium in the crystal lattice. Indenbom and Chernysheva⁶ have shown that the angle of rotation ϕ , of the optical indicatrix because of the spontaneous shear γ_z^0 and the spontaneous polarization P_x^0 may be described by:

$$\phi \approx -30b_{14}P_x^0. \quad (1)$$

The piezoelectric constant b_{14} is essentially the same for both RS and the deuterated salt as shown by Mason and Holden.¹⁰ The dielectric properties are, however, strongly affected as shown by the detailed studies of Hablutzel.¹¹ The Curie temperatures of DRS occur, respectively, at -22°C and $+35^\circ\text{C}$ compared to normal RS whose Curie temperatures are at -18°C and $+23^\circ\text{C}$. In addition, a large increase in spontaneous polarization is obtained which, according to (1), should lead to a greatly enhanced electro-optic effect. DRS also has a somewhat greater secular stability and is less subject to deliquescence and efflorescence than normal RS.

Crystals of DRS were grown at this laboratory by

Parkerson¹² by dissolving desiccated RS in D₂O, a seed crystal being suspended in the saturated solution at $+36.4^\circ\text{C}$ and the temperature dropped at approximately 0.1°C per day. The crystal habit was found to be the same as that of ordinary RS and the orientation of the crystallographic axes was determined by means of x-ray diffraction.

The crystals were diced into tabular plates oriented with respect to the crystallographic axes, the ferroelectric a axis being parallel to the major crystal faces of $2\text{ cm} \times 1\text{ cm}$. In order to keep the number of domains at a minimum,⁵ the crystal thickness was kept relatively large ranging between 0.22 cm and 0.80 cm .

The crystals were ground flat with 600 grit dry silicon carbide paper and polished against a nylon backing with a slurry of glycerine and alumina and thereafter cleaned in alcohol.

Liquid electrodes of saturated solution of DRS in D₂O covered by conductive glass plates were affixed to the major surfaces and held in place by several coats of transparent nail polish applied around the crystal edges and sides to prevent dehydration.

Electric fields were applied to the crystal in the form of pulses of variable amplitude and alternating polarity with a rise time better than 10 millimicroseconds and sufficient duration to polarize the crystal to saturation. All experiments were made at a room temperature of $+25^\circ\text{C}$ the temperature remaining constant to within 1°C .

Motion pictures were taken of nucleation and wall motion of domains through the ocular lens of a polarizing microscope. In each case an area of the crystal was selected which gave reproducible results. Generally this was found to be near one of the crystal edges. The motion picture camera had a clear field of view, approximately $(0.12 \times 0.08)\text{ cm}^2$ of the crystal surface. Figure 1 shows a sequence of motion picture frames which illustrate part of the process of nucleation and wall motion of domains when a pulsed electric field is applied to a single domain crystal of DRS.

Nucleation of a b domain begins apparently at a crystal edge in the xz plane. The domain then appears

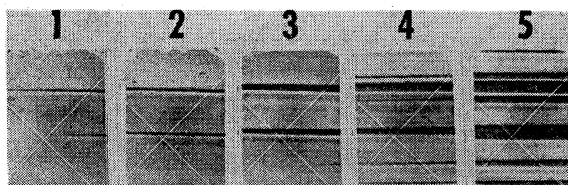


FIG. 1. Nucleation and wall motion of c domains are shown in five sequential motion picture frames taken at 0.125-second intervals. Upon the application of a pulsed electric field domain wedges nucleate at an edge parallel to the crystallographic b axis. Growth of a domain then proceeds in the yz plane while new domains are being nucleated.

⁷ R. Abe, J. Phys. Soc. (Japan) **13**, 244 (1958).

⁸ H. H. Wieder, Phys. Rev. **110**, 29 (1958).

⁹ A. G. Chynoweth, Phys. Rev. **110**, 1316 (1958).

¹⁰ W. P. Mason and A. N. Holden, Phys. Rev. **57**, 54 (1940).

¹¹ J. Hablutzel, Helv. Phys. Acta **8**, 489 (1939).

¹² C. R. Parkerson, Technical Memorandum, U. S. Naval Ordnance Laboratory, Corona (unpublished), available from writer on request.

in the yz plane in the form of a wedge which grows rapidly along its long axis, in the crystallographic c direction and slowly, by sidewise displacement of its boundaries, in the direction of the b axis. Frame 2 shows that while two domains are in the process of expanding, a new nucleus had been generated which thereafter proceeds through the same growth cycle as the other domains. Frames 3, 4, and 5 show further details of nucleation and growth of b domains. In general, polarization reversal appears as a competing process of nucleation and growth of either b domains or c domains. If both b and c domains are present within a crystal, the reversal process is not altered although the number of participating domains increases and nucleation appears as a more significant process than wall motion.

In order to determine whether the domains shown in Fig. 1 may be considered as laminae parallel to the ab plane, the domain structures on opposite crystal faces were compared and found to be essentially the same. The difference in focusing the microscope on a domain edge located at the top and bottom surfaces of the crystal indicated, however, a slight slope of the order of 3° between the a axis and the domain boundary. The velocity of propagation of domain walls in the direction of the ferroelectric a axis could not be determined experimentally. It is to be expected, however, that it is several orders of magnitude faster than propagation along either the b or the c axis.

Quantitative measurements of domain wall displacement as a function of time obtained from motion picture photographs are shown in Fig. 2 for an applied field of 60 volts/cm. The domain wall propagates initially at a relatively constant velocity of the order of 1.6×10^{-3} cm/sec. As two walls approach each

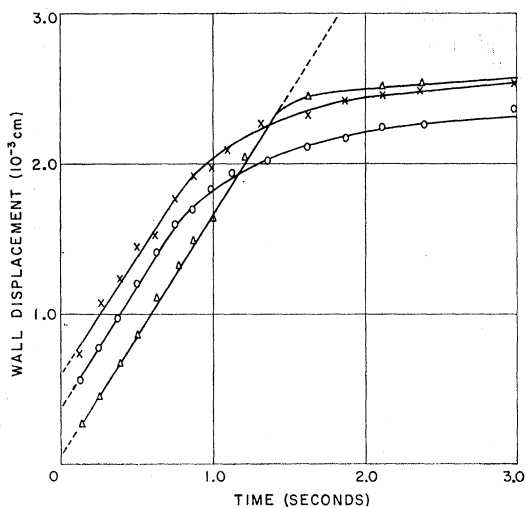


FIG. 2. Displacement of three different domains along the b axis for a field of 60 v/cm. The displacement becomes nonlinear when two walls approach each other. In the linear region the velocity is constant.

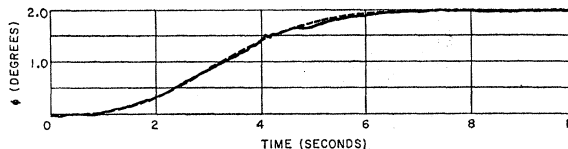


FIG. 3. Solid curve shows the effective rotation of the plane of polarization as a function of time for specimen DRS-1 with $E=60$ v/cm. Dashed curve was calculated by means of Eq. (5).

other, their displacement slows to a logarithmic rate. This is quite reasonable considering that in the region between two walls approaching from opposite directions, large strains are induced generating a corresponding stress which effectively reduces the applied field at the wall. If proportionality between displacement velocity of a domain boundary and this retarding force is assumed, then a sharp decrease in velocity is to be expected.

From photographs such as shown in Fig. 1, it was found that the angle θ , included between a domain wall and the c axis, remained an essentially constant 88° throughout the growth cycle of a domain. If domains are then considered to be essentially parallel to the a axis, then their growth may be represented as a two-dimensional expansion of an isosceles triangle projected on the yz plane. For the sake of simplicity, the propagation velocities along the b and c axes are assumed to be constant by neglecting the decrease in velocity as the wedge tip approaches the opposite crystal boundary as well as the interaction between walls described above. If the displacements along the b and c axes are $2y$ and z , respectively, and $y=v_y(t-\tau)$ where τ is the time at which the domain was nucleated, then since $z=y \tan\theta$, the area s , subtended by a growing domain upon the major crystal surface area S_0 is:

$$s = v_y^2 (t - \tau)^2 \tan\theta. \quad (2)$$

For the purpose of monitoring polarization reversal on a continuous basis, an experimental arrangement similar to that of Abe⁷ was employed, the DRS crystal being mounted between the polarizer and the analyzer of a polarizing microscope and a type 931A photomultiplier fitted at the ocular. Generally, the analyzer was adjusted to within 5° of extinction. The light of a tungsten filament fed from a regulated dc source and passed through a collimator was used to illuminate the crystal.

Alternatively, for viewing the entire crystal surface, a pair of Glan-Thompson prisms set in a rotatable mounting calibrated in 5 seconds of arc were substituted for the microscope. The photomultiplier current induced by the light passing through the crystal is proportional to the fraction of the total number of domains oriented in the direction of the applied field. Plotted as a function of time, this current provides a direct representation of polarization reversal. Figure 3 shows such a plot, the ordinate having been calibrated

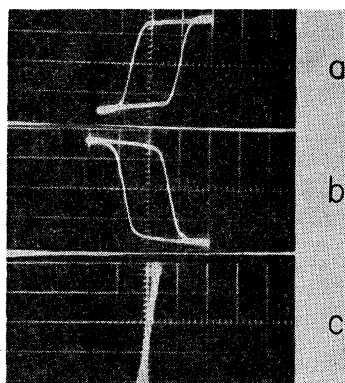


FIG. 4. Electro-optic and dielectric hysteresis and the proportionality between polarization and the electro-optic Kerr effect during polarization reversal. (a) Electro-optic hysteresis loop. Abscissa represents applied field, ordinate, the corresponding current induced in a photomultiplier by polarized light passing through DRS-3. (b) Dielectric hysteresis loop obtained on modified Sawyer-Tower bridge circuit. Ordinate represents polarization, abscissa the electric field. (c) Polarization as a function of electro-optic signal amplitude. It was obtained by applying signals shown on ordinates of 4(a) and 4(b), respectively, to the x and y plates of an oscilloscope.

in terms of the effective angular rotation of the plane of polarization by the compensating rotation of the analyzing prism. The spontaneous polarization of DRS at $+25^\circ\text{C}$ was obtained by Hablutzel¹¹ from hysteresis loop data to be $P_s = 0.3 \mu\text{coulombs/cm}^2$ or $9 \times 10^2 \text{esu/cm}^2$, our own similar measurements agree to within 1% of this value. Since, according to Mason,¹³ $b_{14} = 6.3 \times 10^{-7}$, then from Eq. (1), the spontaneous angle of rotation $\theta_s = 1.70 \times 10^{-2}$ radian or 0.975 degree. This obviously is in very good agreement with the value of $2\theta_s = 2$ degrees shown in Fig. 3.

Is there also direct correspondence between polarization and electro-optic parameters dynamically during reversal? Some evidence for this is shown in Fig. 4. An electro-optic hysteresis loop with the photomultiplier current plotted as a function of field is shown in Fig. 4(a). The corresponding typical ferroelectric hysteresis loop with polarization plotted as a function of field, is shown in Fig. 4(b). In each case an alternating, sinusoidal, 60 cps electric field with a peak value of 400 volts/cm was applied to the same DRS crystal. Figure 4(c) shows the linear relation between polarization and the effective angle of rotation when the crystal is subjected simultaneously to electro-optic and dielectric hysteresis by means of the same ac field. It is obtained when the output of a modified Sawyer-Tower circuit is applied to the y plates and the photomultiplier current to the x plates of an oscilloscope by means of suitable amplifiers.

In view of observations on domain nucleation and growth such as illustrated in Fig. 1, the electro-optic

transients obtained during reversal such as shown in Fig. 3 and the relation $(\Delta\phi/2\phi_s) = (\Delta P/2P_s)$ illustrated in Fig. 4, it seems reasonable to interpret polarization reversal of DRS in terms of the same phenomenological model developed in detail for BaTiO_3 ⁹ and colemanite.¹ The effective rotation of the plane of polarization referred to the fraction of the crystal surface area subtended by nucleated and growing domains may then be written as:

$$\frac{\phi(t)}{2\phi_s} = \frac{1}{S_0} \int_0^t s(t, \tau) \cdot \left(\frac{dN}{dt} \right)_{t=\tau} d\tau. \quad (3)$$

The nucleation rate (dN/dt) is considered to be controlled by a statistical law such as found for other ferroelectrics of the form:

$$(dN/dt) = kN_0 \exp(-kt), \quad (4)$$

where N_0 represents the total number of nucleation sites and k is a nucleation probability factor. From Eqs. (2), (3), and (4) and with due account of the ingestion of some nucleation sites because of the expanding domains, the electro-optic polarization reversal transient may be expressed as:

$$\frac{\phi}{2\phi_s} = 1 - \exp \left[- \frac{2v^2 N_0 \tan\theta}{S_0 k^2} \left(\frac{k^2 t^2}{2} - kt + 1 - e^{-kt} \right) \right]. \quad (5)$$

The nucleation probability factor k , as well as the fraction (N_0/S_0) must be determined from experimental parameters before a comparison may be attempted between (5) and Fig. 3. Since the time derivative of (5) is:

$$\frac{d\phi}{dt} = \frac{2v^2 N_0 \tan\theta}{kS_0} (2\phi_s - \phi)(kt - 1 + e^{-kt}), \quad (6)$$

k may be derived from the slope of $\log(d\phi/dt)$ vs t in the region when $kt \approx 1$.

Individual $(d\phi/dt)$ points were obtained from Fig. 3 by a graphical method such as described by Pearlson

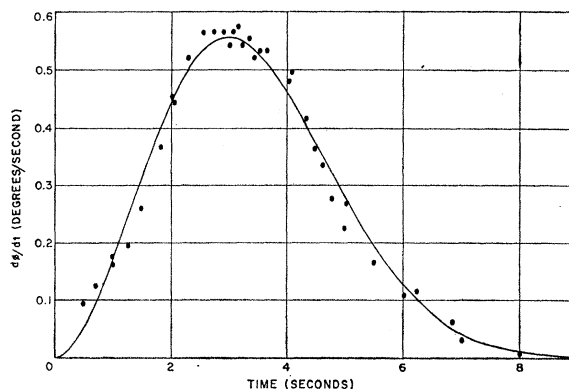


FIG. 5. Graphically determined points $(d\phi/dt)$ from Fig. 3 are shown individually as a function of time. The curve was calculated by means of Eq. (6).

¹³ W. P. Mason, *Piezoelectric Crystals and their Application to Ultrasonics* (D. Van Nostrand Book Company, Inc., Princeton, New Jersey, 1950).

and Simmons¹⁴ and the results are plotted as a function of time in Fig. 5. From the rising portion of the curve shown in Fig. 4, plotted as shown in Fig. 6, the nucleation probability factor is then calculated as $k=1.03$ seconds⁻¹. Upon taking the time derivative of (6) and maximizing the resultant expression, it is found that:

$$\frac{2v^2 N_0 \tan \theta}{S_0} = \frac{1 - \exp(-kt_m)}{[kt_m - 1 + \exp(-kt_m)]^2} = 0.22 \text{ second}^{-2}, \quad (7)$$

since $t_m \approx 3$ seconds may be obtained by inspection from Fig. 5. Theoretical curves of ϕ vs t and $(d\phi/dt)$ vs t , may now be calculated by means of (5) and (6) and the corresponding curves shown in Figs. 3 and 5, illustrate the good agreement obtainable between the parameters of the theoretical model and experimental data.

Equation (7) also permits a rough estimate of the number of nucleation sites per unit surface area since $v \approx 1.6 \times 10^{-3}$ cm/sec and $\tan \theta \approx 28.6$; therefore, $(N_0/S_0) \approx 1.5 \times 10^8$ nucleation sites per cm² of surface area. Now the portion of the crystal surface shown in Fig. 1 is 9.6×10^{-3} cm²; therefore, some fourteen nucleation sites ought to be available within it. Six individual domains are visible and in view of possible ingestion of some of the sites by the growing domains, this seems reasonable.

The theoretical and experimental curves shown in Fig. 5 are qualitatively analogous to the displacement current transients observed during polarization reversal. Such a transient is illustrated in Fig. 7(a). The corresponding theoretical curve was calculated by means of Eqs. (5), (6), and (7). For comparison purposes, Fig. 7(b) shows P vs t obtained graphically from the experimental transient, the close analogy to Fig. 3 being clearly apparent. The switching speed shown in Fig. 7 is, however, nearly twice as fast as that shown in Fig. 5. This is due in part to the fact that different specimens have quite different field dependences for both the electro-optic and switching experiments. DRS crystals also appear to be subject to the same "fatigue effect" dis-

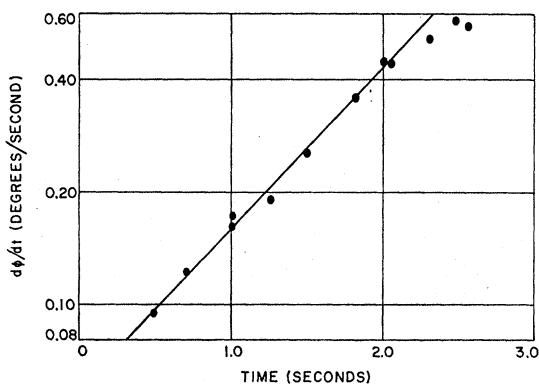


FIG. 6. A plot of $\log(d\phi/dt)$ vs t using the data from Fig. 5, is shown to be a straight line whose slope is $k=1.03$ seconds⁻¹.

¹⁴ W. H. Pearlson and J. H. Simmons, *J. Am. Chem. Soc.* **67**, 352 (1945).

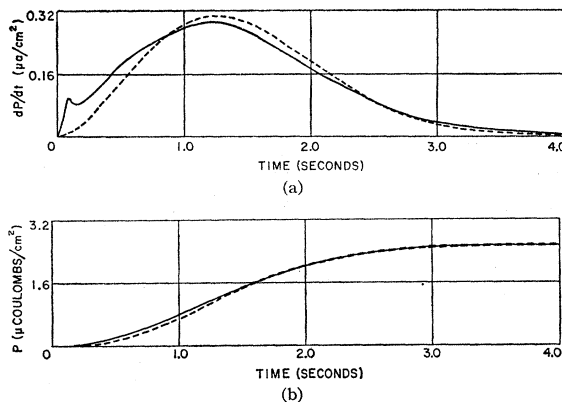


FIG. 7. Experimental and calculated displacement current transients and polarization reversed as a function of time. (a) Solid curve represents experimental displacement current density as a function of time for an applied field of 60 v/cm, sample DRS-2. Dashed curve was calculated from (6) with $k=4$ seconds⁻¹. (b) Polarization reversed as a function of time obtained by graphically integrating displacement transient. Dashed curve was calculated by means of Eq. (5).

cussed by Abe⁷ in the case of RS. Qualitatively, the switching time seemed to decrease exponentially with field in the case of samples in which the fatigue effect was minimized; however, no consistent quantitative field dependence could be obtained for either the electro-optic or the displacement current transients.

In contrast, the characteristic shape and the symmetry of the curves, such as illustrated for both the electro-optic and dielectric transients, was found to be independent of the applied field between 50 volts/cm and 220 v/cm, the upper limit set by the crystal thickness and voltage amplitude of the pulse generator.

Below 60 v/cm the two-dimensional model of polarization reversal no longer applies. Electro-optic transients as well as displacement current transients were found to approach an exponential polarization reversal such as found by Nakamura,¹⁵ of the form:

$$P = 2P_s [1 - \exp(-\beta t)]. \quad (8)$$

The time constant β is field dependent but varied greatly between crystal specimens ranging from a high of $\beta = 5 \times 10^{-2}$ second⁻¹ to a low of $\beta = 2 \times 10^{-3}$ second⁻¹ for $E = 40$ v/cm. From quasistatic hysteresis loop measurements on RS, Nakamura found a relation such as (8) at 62.5 v/cm and +10°C with a value of $\beta \approx 2.8 \times 10^{-4}$ second⁻¹. Electro-optic polarization reversal curves obtained by Abe⁷ also show an exponential dependence of ϕ upon t . At low fields, Nakamura¹⁵ clearly shows by means of the domain pattern in RS, that wall motion plays an insignificant role and the nucleation of new domains is primarily responsible for polarization reversal. Qualitatively this was verified in our experiments; nevertheless, we are unable to confirm the existence of a threshold field, i.e., a true coercivity, for both

¹⁵ T. Nakamura, *J. Phys. Soc. (Japan)* **12**, 477 (1957).

wall motion and nucleation between 220 and 30 volts/cm.

3. DISCUSSION

In spite of gross simplifying assumptions, polarization reversal and the domain dynamics in RS and DRS for $E \geq 50$ volts/cm are adequately described, as shown above, by a phenomenological model based primarily on nucleation and sidewise expansion of domains. A consequence of such a model as shown by White,¹⁶ is that:

$$0.395 \leq P_m/2P_s \leq 0.487, \quad (9)$$

where P_m corresponds to the polarization reversed between $t=0$ and $t=t_m$. From Figs. 3 and 4 the ratio $(\phi_m/2\phi_s)=0.425$ is obviously well within the range of (7) thus providing additional support for the two-dimensional model of reversal. As the applied fields are increased, the number of nucleated domains increase hence their sidewise displacement is likely to play a smaller role in the reversal mechanism. Polarization reversal would then have to be expressed either as a three-dimensional domain growth process or conceivably nucleation and growth in the direction of the ferroelectric axis might provide a satisfactory model for the main part of the process. Partial confirmation for the latter may be found in the relative switching time of RS determined from the displacement current transients⁸ at high fields. The switching time is smaller and the velocity of reversal much greater than the magnitudes extrapolated from our experiments or those of Mitsui and Furuichi.⁵ Evidence of domain growth in the direction of the ferroelectric axis is also available from the experiments of Marutake¹⁷ as well as from the orientation of domains at zero field investigated by Chernysheva.¹⁸ There is reason to suspect, therefore, that no unique mechanism of polarization reversal is valid for Rochelle salt except at low fields in relatively unstressed crystals such as used in the present experiments.

David¹⁹ had shown that the effects of a mechanical stress upon the ferroelectric polarization are equivalent to that of an electric biasing field. It seems reasonable, therefore, to expect that a localized stress will then

decrease the effective field at the wall and hence retard or impede wall motion thus giving rise to a polarization reversal process controlled mainly by the nucleation of new domains. It is likely that the threshold field for both wall motion and nucleation encountered by Nakamura is also due to a form of stress anisotropy since the nucleation probability also depends upon the effective local field.

4. SUMMARY AND CONCLUSIONS

In ferroelectric crystals such as RS and DRS which have a large electro-optic Kerr effect, the spontaneous rotation of the optical indicatrix permits the direct viewing of nucleation and growth of domains and the association of domain dynamics with the displacement current and the polarization reversal process.

The result of optical and electrical experiments using pulsed electric fields above 50 volts/cm confirm a model applied successfully on other ferro-electrics. This model takes into account the nucleation of domains, their growth in two dimensions perpendicular to the ferroelectric axis, and the ingestion of some nucleation sites due to expanding domain boundaries.

Below 50 volts/cm, a localized stress distribution within the crystal hinders wall motion and polarization reversal then takes place mainly by the nucleation of new domains. At high fields, nucleation of domains again predominates because of the large number of nucleated domains and the consequently limited sidewise expansion before coagulation sets in, but growth in the direction of the ferroelectric axis is considered to provide a significant contribution to polarization reversal. The process should then be regarded as one of three-dimensional growth, but since the main contribution probably arises only from nucleation and growth along the a axis, a one-dimensional model should be satisfactory.

Since in general, a crystal of RS or DRS consists of domains oriented along any of the crystallographic axes, no unique model for polarization reversal can be postulated except as in the case of the presently described experiments where a repetitive, self-consistent domain pattern can be obtained in relatively unstressed crystals.

ACKNOWLEDGMENTS

The authors gratefully acknowledge the continued support of the Office of Naval Research during this phase of research on ferroelectrics. We are indebted to C. R. Parkerson for the crystals of DRS, and to D. J. White for many stimulating discussions.

¹⁶ D. J. White, Technical Memorandum 43-40 U. S. Naval Ordnance Laboratory, Corona (unpublished), available from author on request.

¹⁷ M. Marutake, J. Phys. Soc. (Japan) 7, 25 (1952).

¹⁸ M. A. Chernysheva, Izvest. Akad. Nauk S.S.S.R. Ser. Fiz. 2, 289 (1957) [translation: Bull Acad. Sciences (U.S.S.R.) 21, 293 (1957)].

¹⁹ R. David, Helv. Phys. Acta 8, 431 (1935).

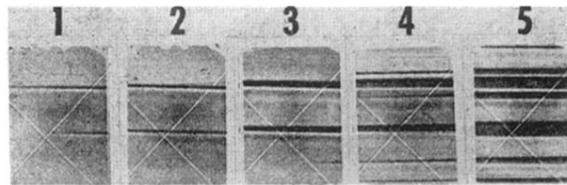


FIG. 1. Nucleation and wall motion of c domains are shown in five sequential motion picture frames taken at 0.125-second intervals. Upon the application of a pulsed electric field domain wedges nucleate at an edge parallel to the crystallographic b axis. Growth of a domain then proceeds in the yz plane while new domains are being nucleated.

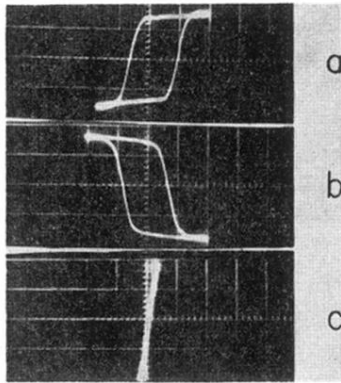


FIG. 4. Electro-optic and dielectric hysteresis and the proportionality between polarization and the electro-optic Kerr effect during polarization reversal. (a) Electro-optic hysteresis loop. Abscissa represents applied field, ordinate, the corresponding current induced in a photomultiplier by polarized light passing through DRS-3. (b) Dielectric hysteresis loop obtained on modified Sawyer-Tower bridge circuit. Ordinate represents polarization, abscissa the electric field. (c) Polarization as a function of electro-optic signal amplitude. It was obtained by applying signals shown on ordinates of 4(a) and 4(b), respectively, to the x and y plates of an oscilloscope.